Biochimica et Biophysica Acta 1848 (2015) 581–592

Contents lists available at ScienceDirect

Biochimica et Biophysica Acta

journal homepage: www.elsevier.com/locate/bbamem

Molecular dynamics methods to predict peptide locations in membranes: LAH4 as a stringent test case

A. Farrotti [a], G. Bocchinfuso [a], A. Palleschi [a], N. Rosato [b,c], E.S. Salnikov [d], N. Voievoda [d], B. Bechinger [d], L. Stella [a,*]

[a] Dipartimento di Scienze e Tecnologie Chimiche, Università di Roma "Tor Vergata", 00133, Rome, Italy
[b] Dipartimento di Medicina Sperimentale e Chirurgia, Università di Roma "Tor Vergata", 00133, Rome, Italy
[c] NAST center, Università di Roma "Tor Vergata", 00133, Rome, Italy
[d] Université de Strasbourg/CNRS, Institut de Chimie UMR7177, F-67000, Strasbourg, France

ARTICLE INFO

Article history:
Received 2 September 2014
Received in revised form 22 October 2014
Accepted 5 November 2014
Available online 13 November 2014

Keywords:
Membrane-active peptides
Molecular dynamics simulations
Coarse grained force fields
Potential of mean force
Solid-state NMR

ABSTRACT

Determining the structure of membrane-active peptides inside lipid bilayers is essential to understand their mechanism of action. Molecular dynamics simulations can easily provide atomistic details, but need experimental validation. We assessed the reliability of self-assembling (or "minimum-bias") and potential of mean force (PMF) approaches, using all-atom (AA) and coarse-grained (CG) force-fields. The LAH4 peptide was selected as a stringent test case, since it is known to attain different orientations depending on the protonation state of its four histidine residues.

In all simulations the histidine side-chains inserted in the membrane when neutral, while they interacted with phospholipid headgroups in their charged state. This led to transmembrane orientations for neutral-His LAH4 in all minimum-bias AA simulations and in most CG trajectories. By contrast, the charged-His peptide stabilized membrane defects in AA simulations, whereas it was located at the membrane surface in some CG trajectories, and interacted with both lipid leaflets in others. This behavior is consistent with the higher antimicrobial activity and membrane-permeabilizing behavior of the charged-His LAH4. In addition, good agreement with solid-state NMR orientational data was observed in AA simulations.

PMF calculations correctly predicted a higher membrane affinity for the neutral-His peptide. Interestingly, the structures and relative populations of PMF local free-energy minima corresponded to those determined in the less computationally demanding minimum-bias simulations.

These data provide an indication about the possible membrane-perturbation mechanism of the charged-His LAH4 peptide: by interacting with lipid headgroups of both leaflets through its cationic side-chains, it could favor membrane defects and facilitate translocation across the bilayer.

1. Introduction

Several peptides exert their functions by interacting with cell membranes. Based on their effect, these membrane-active peptides are usually divided in different classes. Host-defense peptides are a heterogeneous class of amphipathic oligopeptides, which kill pathogens, and even cancerous cells, mainly by inducing leakage of their cell membranes through physical interactions with the lipid bilayer, making these molecules promising compounds to fight drug-resistant bacteria [1–3]. Cell-penetrating peptides (CPPs) are used to deliver therapeutic molecules (nucleic acids, drugs, imaging agents) to cells and tissues in a nontoxic manner [4,5]. In the case of amyloid peptides the mechanisms of aggregation and toxicity are not fully understood, but a common property of these peptides is their ability to interact with lipid bilayers, thereby disturbing membrane integrity. Lipid bilayers can also act as conformational catalysts, favoring protein misfolding and aggregation [6]. Fusion peptides are segments of viral proteins, or model oligopeptides, with the ability to facilitate the merging of two apposed lipid bilayers, a fundamental event in many biological processes [7]. Finally, other peptides are able to recognize membrane regions with a specific curvature, or to deform lipid bilayers [8]. Notably, many peptides exhibit various functionalities and the separation into distinct classes is not always obvious [9].

The molecular details of the mechanism of action of many of these systems are still debated. This deficiency is due mainly to the difficulties involved in the application of atomic-resolution structural techniques (X-ray crystallography and NMR spectroscopy) to membrane systems.

Abbreviations: PMF, potential of mean force; AA, all-atom; CG, coarse-grained; MD, molecular dynamics; CPP, cell-penetrating peptide; FF, force-field; ATR-FTIR, attenuated total reflection Fourier-transform IR; OCD, oriented circular dichroism; TM, transmembrane; LAH4-c, charged His LAH4; LAH4-n, neutral His LAH4; POPC, 1-palmitoyl-2-oleoyl-*sn*-glycero-3-phosphocholine; POPS, 1-palmitoyl-2-oleoyl-*sn*-glycero-3-phospho-L-serine; SW, standard water; PW, polarizable water; COM, center of mass; WHAM, weighted histogram analysis method

* Corresponding author.
E-mail address: stella@stc.uniroma2.it (L. Stella).

http://dx.doi.org/10.1016/j.bbamem.2014.11.002
0005-2736/

Although significant advances are being achieved in these areas [10,11] determination of the structure, position and orientation of peptides and proteins in membranes is still a challenge, in particular as the outlines of the lipid bilayers in or from high-resolution structures often remain purely speculative. For this reason, alternative approaches are of particular interest to study peptide–lipid interactions.

Molecular dynamics (MD) simulations can provide atomic-level data on the structure and dynamics of peptide–membrane systems [12,13]. However, they might be affected by the approximations used in the computation of the trajectories or suffer from sampling and convergence problems due to the limited length of the simulations, typically in the 0.1–1 μs time-range. For instance, the simplest, brute force approach follows the motions of all atoms in the system without any external perturbation ("unbiased simulations"), starting with a preformed bilayer and with the peptide in the water or in the membrane phase. In these cases, relaxation to the minimum free-energy configuration and peptide conformation often does not take place during accessible time-scales, due to the relatively viscous and ordered membrane environment [14–17]. Therefore, the "unbiased" attribute might be misleading for these simulations of membrane systems, since the final results are significantly affected by the starting conditions (even though technically the term "unbiased" refers to the absence of external perturbations to the system).

A common method to increase the accessible simulation time is based on the so-called coarse-grained (CG) force fields (FFs) [18]. In CG simulations, groups of atoms are treated as a single particle (bead), thus reducing the degrees of freedom of the system. The loss of atomic details is balanced by an increase in sampling of up to 4 orders of magnitude, in comparison with AA simulations [19]. For this reason, CG FFs, and particularly MARTINI, are widely applied to peptide–membrane systems, although the approximation used for water molecules has been consistently shown to disfavor the formation of membrane defects or pores [20]. In addition, also for these kinds of FFs, "unbiased" simulations starting from preformed bilayers might fail to determine the correct peptide position/orientation in the membrane, because the system is caught in a local free-energy minimum [21].

To solve problems related to the slow relaxation of membrane systems, we [2,22,23] and others [18,24–28] have used an approach that we termed "minimum bias", since it minimizes the effect of the initial configuration on the final results. In this method, which has been applied to both AA and CG FFs, the simulation is started from a random mixture of peptide, lipids and water, and the bilayer forms spontaneously in 50–100 ns. During this self-assembly process, the system is much more fluid than a fully formed bilayer, especially in the first stages of the simulation. This ensures that the peptide can experiment different environments in a relatively short time, and, as a consequence, it is more likely to find its minimum free energy configurations. Notably, this approach is similar to many biophysical experiments, such as solid-state NMR, attenuated total reflection Fourier-transform IR (ATR-FTIR) or oriented circular dichroism (OCD), where membranes are formed from lipid–peptide mixtures completely dissolved in organic solvents [29].

Another method to improve sampling of the system configurations involves the addition of restraints to pull the peptide from the water solution to the center of the bilayer. By performing several independent simulations with the peptide placed at different depths, it is possible to determine the potential of mean force (PMF), or free-energy profile, as a function of peptide position in the membrane. PMF calculations have been successfully applied to determine the position and conformation of peptides in lipid bilayers [17,30–32]. In addition, PMF analyses give a picture of the whole insertion pathway, including the configurations corresponding to the potential energy barriers to the insertion, or to local minima. However, the need to attain an equilibrated system at each depth of peptide insertion [32] makes PMF calculations rather demanding, so that CG FFs are often used to reduce the computational costs [21,33,34].

In this article we aim to assess the reliability of the "minimum bias" (AA and CG) and CG PMF approaches, by comparing their results with experimental data. To this end, an ideal test case is provided by the designed peptide LAH4, which exhibits both antimicrobial and cell-penetrating activities [35,36]. Its sequence (KKALLALALHHLAHLALH LALALKKA-NH_2) comprises four histidines in the central part, which in micelles exhibit pK_a values between 5.4 and 6.0, so that the total peptide charge can be tuned in a pH-dependent manner [37]. NMR, ATR-FTIR and CD experiments demonstrated that LAH4 is predominantly helical when membrane bound, with an amphiphilic distribution of the His and Leu/Ala side-chains [38–40]. In POPC membranes, the peptide helix changes its orientation together with the protonation state of the His residues, going from a prevalently in-plane to a transmembrane (TM) arrangement when the pH increases from acidic to neutral/basic values [37,38,41].

Although some previous studies compared solid-state NMR experiments with peptide orientations independently predicted from MD simulations [42,43], this is the first article focusing on a single peptide that can sample the different positions/orientations usually observed for membrane-active peptides, simply by varying its protonation state. While this study was in progress, a simulation of LAH4 interaction with membranes was published [44]. However, in that case the simulations were started with a preformed bilayer and the peptide in the water phase, and LAH4 remained associated to the membrane surface, mostly above the phospholipid headgroups, likely due to the problems of convergence affecting this kind of "unbiased" simulations (see above). Our study also offers the additional benefit of comparing different computational approaches (AA and CG minimum bias simulations and CG PMF calculations), so that the advantages and limitations of each method can be discussed. Finally, the computational results can be used to provide an atomic level insight into the mechanisms of membrane activity of LAH4. This peptide has a strong bactericidal activity both at acidic and neutral/basic pH values, but it is more active and membranolytic when its His residues are charged [36,39]. A stronger lytic activity of the charged-His peptide state (LAH4-c, henceforth) has been observed also in model POPC bilayers, even though the neutral-His peptide (LAH4-n) has a higher membrane affinity [39,45].

LAH4 exhibits also an interesting ability to facilitate the entry of nucleic acids into cells, which is correlated with the change in endosomal pH during the transfection process [35,46]. Interaction of DNA with charged peptide residues favors its condensation, while protonation of the His side-chains in the acidic environment of endosomes, and thus activation of the peptide membrane permeabilization activity, favors the escape of nucleic acids to the cytosol [35,47]. However, notwithstanding many studies and several successful practical applications of LAH4 and its analogues in transfection [48,49], the molecular details of their membrane-perturbing activities still need to be clarified.

2. Methods

2.1. AA simulations

AA simulations of LAH4 were performed using the "minimum-bias" method, as previously described [22,24], except for the details reported below. LAH4 was modeled into an α-helix structure and placed at the center of a $9 \times 9 \times 9$ nm box. POPC was selected for forming the membrane since this is the lipid used in the experimental determination of peptide orientation [37,38]. 128 POPC molecules with different conformations [22] and 7500 water molecules were randomly added into the box. Finally, 5 or 9 chloride ions (depending on the protonation state of LAH4 His residues) were introduced in replacement of water molecules to neutralize the system. Similarly to our previous studies of peptide–membrane systems [2,13,22], simulations were performed with the ffgmx force field, implemented with the previously reported parameters for POPC [50], using the GROMACS 4.5 software package [51]. A control box without the peptide and a total of five LAH4

containing systems were assembled and simulated independently. Each system was energy-minimized and then equilibrated using a 100 ps MD simulation where the position of the peptide was restrained. Production simulations were performed for 125 ns at 300 K, followed by annealing cycles between 300 K and 375 K (which were not needed for the simulation without peptide). During each cycle, the temperature was risen from 300 K to 375 K in 2 ns, decreased back to 300 K in 50 ps, followed by 1 ns of simulation at 300 K. If needed, another annealing protocol was employed, in which the temperature was increased in 0.5 ns, kept constant at 375 K for 20 ns and finally brought back to 300 K in 0.5 ns. A final 25 ns simulation at 300 K was performed on the systems with no defects in the bilayer. During this time, no evidences of further significant changes were observed, so that the last 20 ns of each simulation were used for analysis.

2.2. CG simulations

CG simulations were performed using the MARTINI force field, with its extension to proteins [52]. In this representation, groups of four atoms of lipids and amino-acids are mapped into CG beads of four main types (polar, apolar, nonpolar, and charged), with different polarities, van der Waals interaction parameters and hydrogen-bonding capabilities. Bonds between beads are described by harmonic spring potentials and backbone conformations are restrained by using dihedral angle potentials. CG water comprises four real water molecules, described as a single particle (standard water, or SW) [53] or using a three-bead model (polarizable water, or PW) [54]. The "minimum-bias" method was employed again, performing simulations on random mixtures of the peptide, 128 POPC molecules, 1875 CG water beads (SW or PW), and 5 or 9 chloride counterions. The secondary structure of the peptides was restrained in a canonical α-helix structure with a 400 kJ mol^{-1} force constant, except where stated otherwise. 30 independent simulations, 120 ns long, were performed for both protonation states of LAH4 His residues, using SW or PW. Analyses were performed on the last 20 ns of the simulations. MD parameters are summarized in Table S1, and were selected according to the original references of the two different water models. Actual simulation time lengths were multiplied by a conversion factor equal to 4, to take into account the speed up in lateral diffusion coefficients of lipids and TM peptides [20].

2.3. PMF calculations

The energy for the insertion of LAH4 in a lipid bilayer was evaluated by PMF calculations, using the umbrella sampling protocol [55]. Three independent sets of calculations were performed for both protonation states of the LAH4 His residues, each including 97 independent CG simulations, in which the peptide center of mass (COM) was restrained at a specified distance from the bilayer COM (every 0.1 nm from +4.8 nm to −4.8 nm along the axis normal to the bilayer). A force constant of 1000 kJ mol^{-1} nm^{-2} was imposed only on the peptide COM, and LAH4 was free to rotate around it. Simulations were performed with the peptide placed at different positions in a box containing 128 POPC molecules in a preformed bilayer and about 5500 CG water beads, with an initial orientation of the peptide helix parallel to the membrane normal. The protocol used for peptide insertion in the box was the same that we introduced previously for another peptide [13], while MD parameters were set as in the CG simulations with SW (Supplemental Table S1). The boxes were first equilibrated using an annealing process, with the temperature gradually being increased from 50 K to 300 K in 60 ns, and then simulated for 400 ns at 300 K. PMF was calculated with the weighted histogram analysis method (WHAM) [56], using 50 bins and a tolerance of 10^{-6} kJ mol^{-1}. Obtained profiles were finally symmetrized with respect to the bilayer center by using the *g_wham* GROMACS tool. Convergence of the PMF calculations was checked by comparing the three different replicas of each system, and by calculating the free energy profiles as a function of simulation time. For the final analysis, the last 40 ns of each simulation were considered.

2.4. Computation of peptide orientations compatible with the solid-state NMR chemical shifts

To evaluate the peptide orientations that agree with the previously published experimental solid-state NMR spectra of [^{15}N-Ala13]- and [^{15}N-Ala16]-labeled LAH4 [37,41] we followed a protocol already employed in previous studies [57], with some modifications, as here we analyzed the alignment of the plane defined by the peptide bond rather than the orientation of the peptide helix. This approach has the advantage of allowing comparison with the MD simulations of the orientations of the Ala13 and Ala16 sites each individually, thereby avoiding the need to assume a specific peptide structure. The orientation relative to the membrane normal of the plane of the peptide bond (involving the labeled residue and the preceding carbonyl) was defined by two angles, called tilt and pitch (Supplemental Figure S1 A). The tilt is the angle formed by the N–H bond with the normal to the bilayer plane (coincident with the direction of the NMR magnetic field B_0), in the counterclockwise direction. Pitch takes into account rotations of the labeled residue around the N–H bond. Its value is defined as the angle formed by the plane of the peptide bond involving the labeled N atom (plane α) with the plane determined by the bilayer normal and the N–H bond (plane β), counted in a counterclockwise direction. 0° pitch corresponds to the orientation where the carboxyl C atom of the peptide bond lies in plane β (Supplemental Figure S1 B).

The ^{15}N chemical shift of the ^{15}N labeled Ala13 and Ala16 sites was calculated for every possible tilt and pitch value (50 × 50 steps) [57], using the ^{15}N chemical shift main tensor elements (in ppm: 56, 81, 223) and orientations of these main tensor elements within the molecular frame that have been published and analyzed previously (reviewed in [58]).

Contours reported in the so-called restriction plots (Fig. 3) mark the angular restrictions that agree with the experimental ^{15}N chemical shifts by also taking into account an experimental uncertainty of ±5 ppm. From these data, the ranges of tilt angles that (with different pitch values) are consistent with the experimental data were determined. Other possible errors arising from the variance observed during the determination of the ^{15}N chemical shift tensor elements [58] are small when compared to the extended range of acceptable tilt angles defined from a single ^{15}N chemical shift. Due to the symmetries of the system, tilt is reported in the 0°–90° range only.

3. Results

3.1. AA minimum-bias simulations

Initially, we performed two independent AA self-assembling simulations for each protonation state. Fig. 1 shows some representative timeframes along these trajectories. Simulations started from a random mixture of lipids, water and peptide, which was initially placed in a canonical alpha helix conformation. A phase separation occurred relatively quickly (~10 ns), and was followed by a lipid reorganization into a bilayer (~60 ns), which still contained defects and water molecules. Interestingly, from the initial stages of the simulation, neutral His residues were already located in the hydrophobic phase, while charged side-chains were associated to lipid headgroups and water molecules.

Usually, a relatively mild annealing protocol (see Section 2) is sufficient to obtain a perfectly ordered membrane [2,22]. This was indeed the case for simulations of LAH4 with neutral His residues (LAH4-n henceforth), where annealing was started at 125 ns, and all defects were healed after a total time of approximately 230 and 350 ns, in the two simulations. The system was then simulated for further 25 ns at constant temperature.

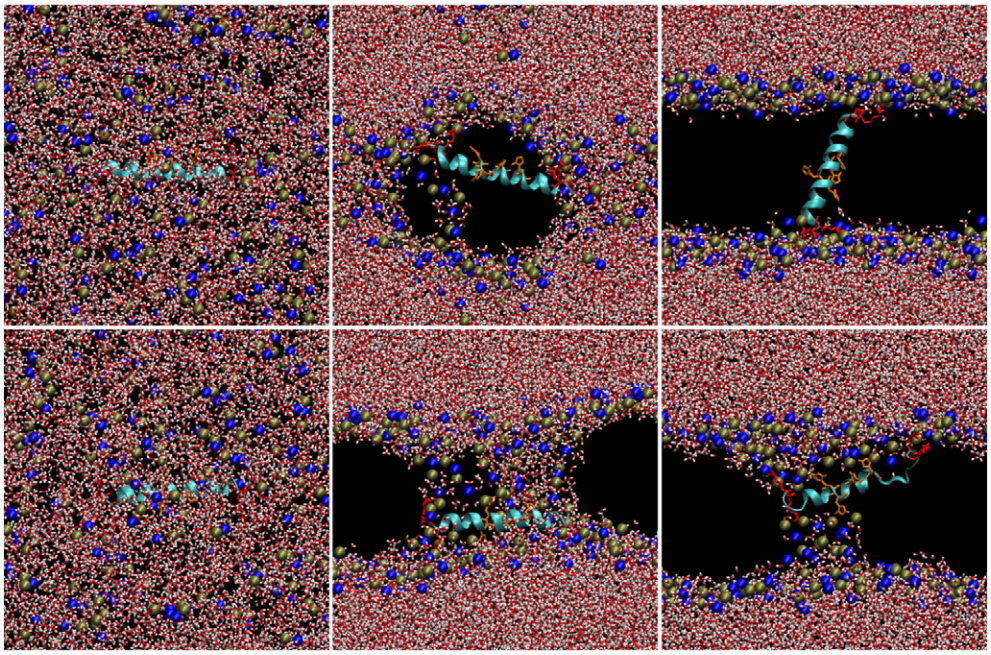

Fig. 1. Snapshots of bilayer formation during LAH4-n (upper panels) and LAH4-c (lower panels) minimum-bias AA simulations. The initial situation (left panels) rapidly evolves into micellar-like clusters, that coalesce to form a bilayer which still contains some defects (middle panels, 50 ns),eventually healed (for LAH4-n) by using an annealing protocol, leading to a defect-free bilayer. Structures at the end of the simulations are reported in the right panels (377 ns and 431 ns for LAH4-n and LAH4-c, respectively). LAH4 is represented as a cyan ribbon, with Lys (red) and His (orange) residues in stick representation. Lipid phosphorus and nitrogen atoms are shown as gold and blue spheres, respectively, while the lipid acyl chains are omitted for clarity. Water molecules are displayed as sticks, with oxygen in red and hydrogen in white.

By contrast, in the case of LAH4 with charged His residues (LAH4-c), it was not possible to remove the membrane defects in either of the two trajectories up to more than 410 ns of simulation time, even annealing the system by maintaining temperatures of 375 K for several periods of 20 ns. To confirm this finding, we performed an additional simulation of LAH4-c, which indeed exhibited a behavior similar to the first two trajectories.

The final structures of all five independent simulations are reported in Fig. 2. In both the LAH4-n trajectories, the peptide attained a transmembrane (TM) orientation, with the His residues located in the hydrophobic core of the membrane. By contrast, the LAH4-c peptides oriented approximately parallel to the membrane surface, and at a shallower depth (Table 1), but some of the charged side-chains interacted with the phosphates of the other leaflet of the bilayer, causing distortions in the peptide helix, and stabilizing the membrane defects and water insertion.

Solid-state NMR data for [^{15}N-Ala13]-labeled LAH4 reconstituted into uniaxially oriented POPC bilayers, showed a distribution of

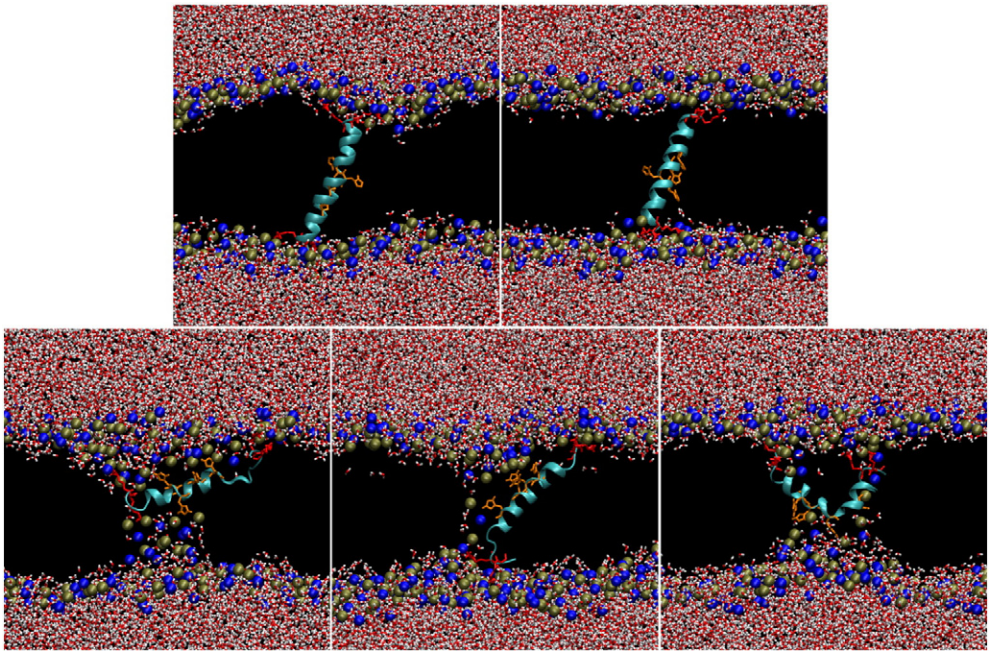

Fig. 2. Final structures obtained for the five AA simulations of LAH4-n (upper panels) and LAH4-c (lower panels).

Table 1
Peptide position and orientation calculated in the last 20 ns of the AA trajectories.[a]

Peptide state	Distance from bilayer center (nm)		Range of tilt angles relative to the bilayer normal (deg)				Amide I order parameter	
	Peptide	His imidazole rings	Ala13 NH		Ala16 NH			
			NMR	MD	NMR	MD	ATR-FTIR	MD
LAH4-n	0.25 ± 0.11	0.15 ± 0.10	0–33	17–33	8–24	20–42	0.55	0.45 ± 0.08
LAH4-c	0.48 ± 0.19	0.60 ± 0.35	49–90	50–90	49–90	50–80	−0.12	−0.1 ± 0.2

[a] ± values or angle ranges represent standard deviations, except for the experimental values, where they are maximum statistical errors. Amide I order parameters were estimated in the simulations from the order parameters of backbone CO bonds (with respect to the bilayer normal).

chemical shifts centered at 70 ppm (±5 ppm) at acidic pH and at 215 ppm (±5 ppm) when the oriented samples were prepared under neutral conditions [37,59]. Similar values of the chemical shifts were observed for [^{15}N-Ala16]-labeled LAH4 under comparable experimental conditions [41]: 80 ppm (±5 ppm) at acidic pH and a main peak at 225 ppm (±5 ppm) under neutral conditions. As already mentioned in Section 1, these data are indicative of a pH-sensitive topological transition from the in-planar to the transmembrane configuration. In order to quantitatively compare this experimental result with the MD simulations, the combinations of tilt and pitch angles of the N–H bond of the labeled amino acids that agree with the observed chemical shift values were calculated following previous protocols [57] (Fig. 3). The ranges of tilt angles that, with different rotational pitch angles, are consistent with the experimental data for LAH4-c and LAH4-n, are reported in Table 1. These values agree, within experimental errors with those observed in the simulations (Table 1).

The orientational transition of LAH4 was observed experimentally also by polarized ATR-FTIR measurements [38], from the order parameters of the amide I transition dipoles, which varied from −0.12 for LAH4-c to 0.55 for LAH4-n. Since the amide I transition is essentially due to stretching vibrations of backbone CO bonds, we calculated the order parameters for these groups in the AA simulations (Table 1). Also in this case, quantitative agreement was observed between experimental data and the simulations.

Another comparison could be performed on the peptide effects on lipid order. The perturbation of deuterium order parameters by LAH4 or its analogues have been measured in a number of different systems, such as POPC, POPC/cholesterol, POPC/POPS/cholesterol 3/1 [60–62 and unpublished data]. Consistently, a larger disordering of the lipid fatty acyl chains has been observed for the in-plane oriented peptide when compared to the transmembrane configuration. A similar trend was observed in our simulations, as an obvious consequence of the defects present in the membranes containing LAH4-c (Fig. 4).

3.2. CG minimum-bias simulations

CG FFs are significantly less demanding than AA simulations in terms of computational resources. Therefore, in this case we could perform 30 independent simulations for each peptide state. Each trajectory was only 120 ns long, because in this case a defect-free bilayer formed in all cases within 100 ns, without the need for any annealing protocol. We also tested several different conditions (see below), including varying degrees of restraints on the peptide secondary structure and two different water models, namely standard (SW) [53] and polarizable water (PW) [54]. In the present system, the CG approach lowered the number of CPU hours per ns with respect to AA simulations by a factor of 1400 or 120, depending on the specific water model used (SW or PW, respectively).

For both LAH4-n and LAH4-c, final structures of the CG simulations showed the peptide either associated to one membrane surface, or interacting with both leaflets. However, in the case of LAH4-n, a clear prevalence of TM states (~75%) was observed with both water models (Table 2). By contrast, under all simulation conditions tested, the two peptide arrangements were observed with approximately equal

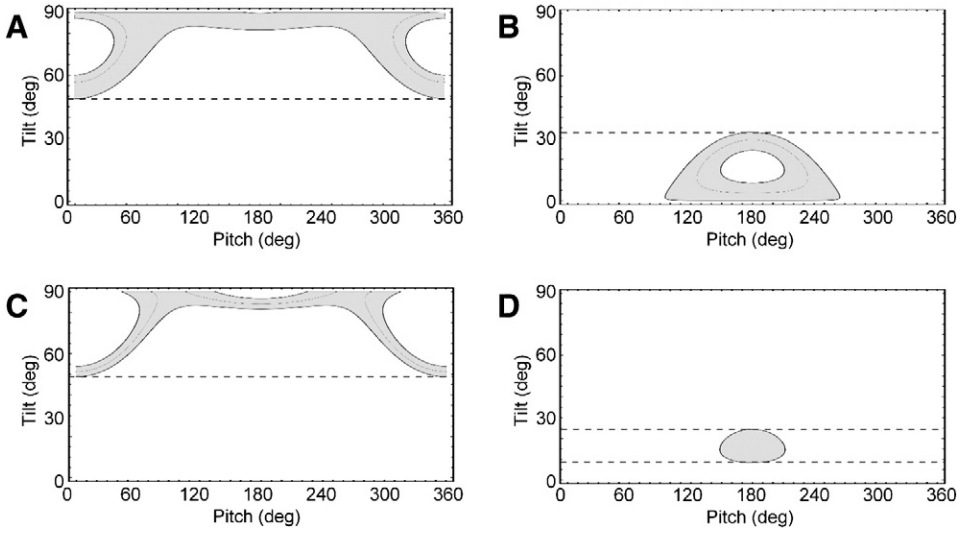

Fig. 3. Restriction analysis of ^{15}N solid-state NMR chemical shift measurements of [^{15}N-Ala13]-LAH4 and [^{15}N-Ala16]-LAH4 in uniaxially aligned POPC bilayers. The alignments of the peptide bond plane that agree with measured ^{15}N chemical shifts are plotted by taking into account ^{15}N chemical shift tensor values (in ppm: 56, 81, 223) and orientations reviewed earlier [58]. Panels A and B: [^{15}N-Ala13]-LAH4 at acidic pH (observed chemical shift 70 ± 5 ppm) and at neutral conditions (215 ± 5 ppm), respectively. Panels C and D [^{15}N-Ala16]-LAH4 at acidic pH (80 ± 5 ppm) and at neutral conditions (225 ± 5 ppm), respectively. In contrast to previous publications the alignments of ^{15}N–H vectors rather than of helical structures are shown (cf. Figure S1 and Section 2).

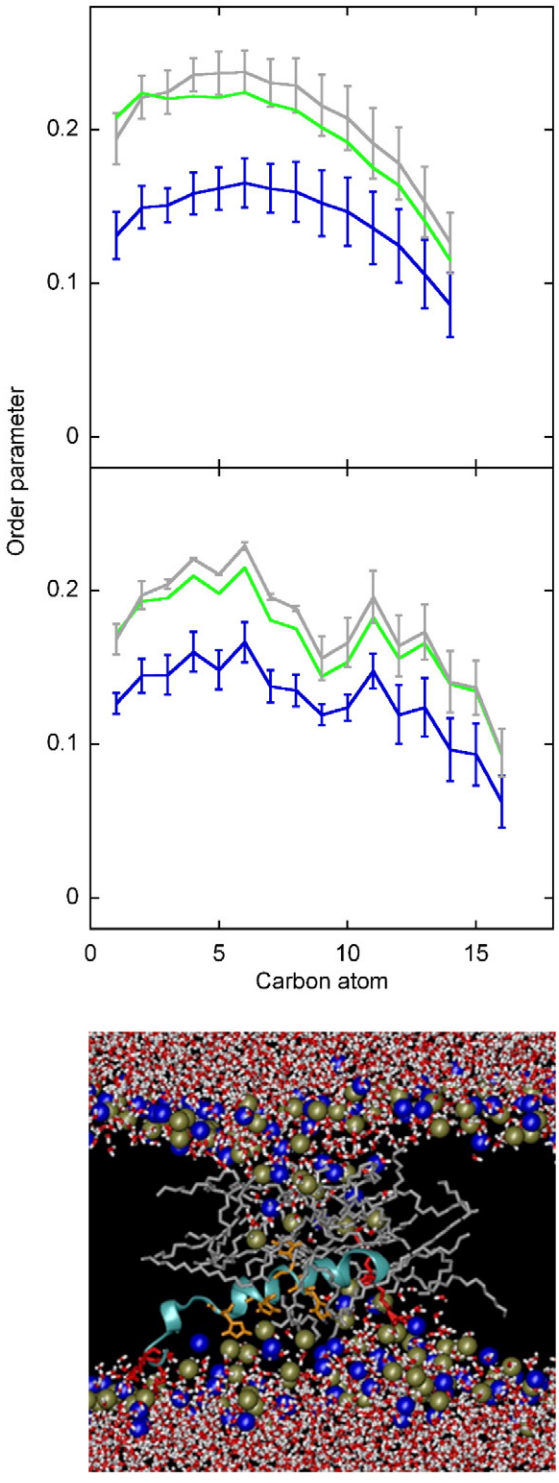

Fig. 4. Peptide effects on lipid order. Deuterium order parameter (C–D) for the palmitic (top panel) and oleic (middle panel) chains in AA simulations. Values were determined in the last 20 ns of trajectories without the peptide (green line), or with LAH4-n (gray) or LAH4-c (blue). Data of peptide-containing bilayers are expressed as the average with standard deviations calculated on all the independent simulations performed. Bottom panel: final structure of one of the LAH4-c AA simulations. The lipid tails of the POPC molecules whose headgroups were stabilized by the peptide at the level of the otherwise hydrophobic core of the membrane are shown as gray sticks.

probability in the case of LAH4-c. Changing the initial conformation of the peptide from perfectly helical to the NMR structure determined in micelles (PDB ID: 2KJN) [40], to the conformation obtained in the AA simulations, or to a manually built perfectly amphiphilic helical conformation, did not modify this finding. Similarly, the two arrangements remained approximately equally populated when the restraints on the backbone dihedrals were removed or rigidified, by increasing the force constant from the standard 400 kJ mol^{-1} value to 1000 kJ mol^{-1}. Extending the simulations (up to 400 ns) after formation of a defect-free bilayer, or performing several annealing cycles, we did not observe any rearrangement of the peptide orientation (data not shown).

Table 2
Peptide orientation in CG minimum bias simulations.

CG water model	Simulations performed	Total time (ns)[a]	% inserted structures[b]
LAH4-n			
SW	30	3600	73
PW	30	3600	77
LAH4-c			
SW	30	3600	53
PW	30	3600	55
PMAP-23			
SW	30	3600	30
Magainin			
SW	30	3600	31

[a] Total times refer to the sum of all trajectory lengths.
[b] Defined as the final arrangements where the peptide was interacting with headgroups of lipids belonging to both leaflets.

As a control, we performed additional simulations with two other cationic peptides (magainin and PMAP-23), for which a surface-bound orientation is distinctly favored, as shown by ^{15}N solid-state NMR [63] and fluorescence measurements [22]. In these cases, peptide arrangements specifically interacting with the headgroups of only one membrane leaflet clearly prevailed in the simulations (Table 2).

It is worth mentioning that the LAH4-c structures in which the peptide interacts with both leaflets through its charged residues are profoundly different from those of LAH4-n (Fig. 5). The neutral-His peptide attains a classical TM arrangement; by contrast, LAH4-c is closer to one membrane surface, with most of the peptide chain oriented parallel to the membrane, and with just the terminal charged Lys residues interacting with the other leaflet of the bilayer. These configurations resemble the structure found in one of the AA simulations (Fig. 2). This finding is demonstrated quantitatively in Fig. 6, showing that LAH4-c is farther from the bilayer center than LAH4-n when in an inserted orientation. This is a consequence of the fact that LAH4-c His residues are always in contact with lipid headgroups, while they are inserted in the core of the membrane for TM LAH4-n.

In the Martini CG FF, a single bead represents backbone atoms. We approximated the N–H bond orientation in the Ala13 and Ala16 regions by considering the vector joining backbone beads of residues -2 and $+2$ with respect to the labeled amino acid, to take into account the $i \rightarrow i + 4$ periodicity of the alpha helix. The angle distributions are reported in Fig. 6, and show a qualitative agreement with NMR data, with LAH4-c forming higher angles with the bilayer normal than LAH4-n.

3.3. CG PMF calculations

In order to assess more quantitatively the free-energy profile for the equilibrium between the superficial and inserted states of LAH4, we performed PMF calculations for peptide insertion into the membrane. Since this type of calculations is rather expensive computationally, we focused on the CG FF, using SW (since the PW model had yielded similar results but at a computational cost more than tenfold higher) and a helical structure for the peptide (since secondary structure restraints did not significantly influence the results of minimum bias CG simulations). Three independent determinations of the free energy profiles as a

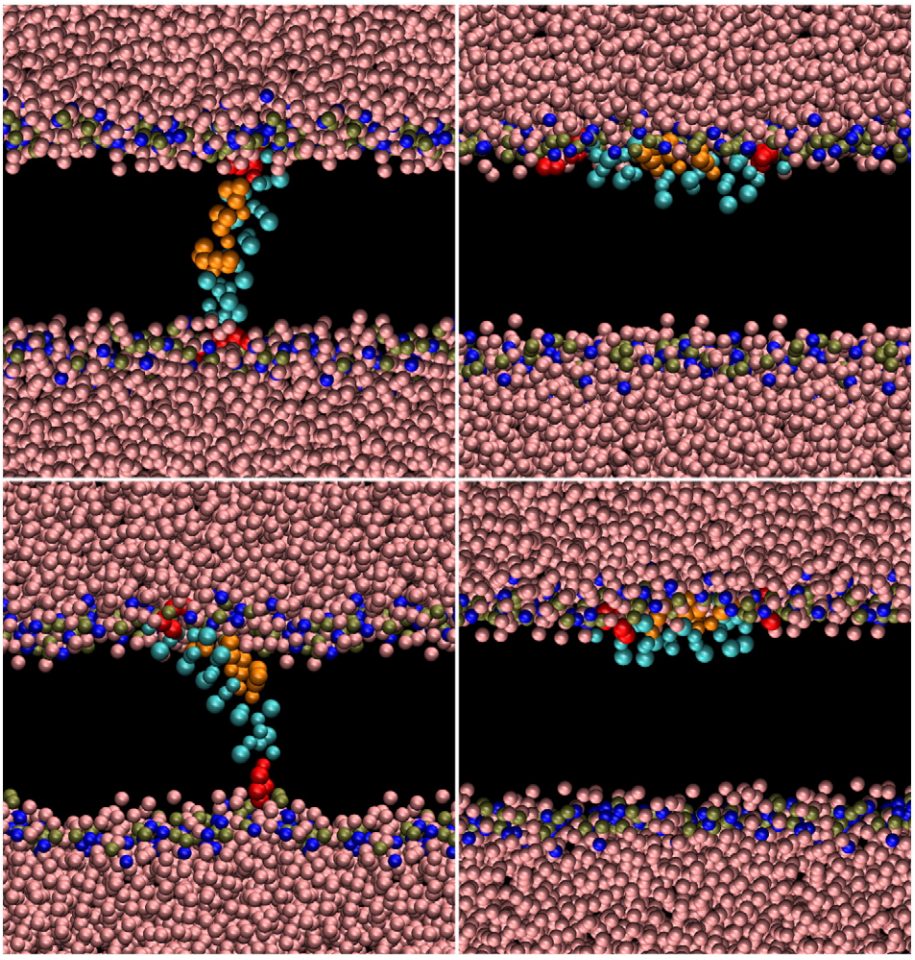

Fig. 5. Final structures in SW CG simulations, representative of the two possible orientations of LAH4-n (upper panels) and LAH4-c (lower panels). The superficial orientation (right) is similar in both the protonation states. On the contrary, in structures with the inserted peptide (left), LAH4-c is more distant from the bilayer center than LAH4-n. The color code is the same of Fig. 1, except for water beads, here shown as pink spheres.

function of peptide distance from the bilayer center were performed for each His protonation state (Supplemental Figure S2). The free energy profile was very similar for all three simulations of LAH4-n, while the relative free-energy of the inserted and superficial states of LAH4-c showed some variation in the different trajectories, indicating a very delicate orientational equilibrium. In any case, convergence of the PMF calculation was attested by the free energy values calculated in different windows of the simulations (Supplemental Figure S3).

The average free energy profiles are reported in Fig. 7, together with the helix tilt angles sampled at each depth of insertion. The PMF calculations predicted a deep minimum for LAH4-n, located in the center of the bilayer. By contrast, this position corresponded to a maximum for LAH4-c, whose free energy profile exhibited minima corresponding to inserted, but more superficial positions. Both protonation states exhibited local minima corresponding to a surface-bound peptide position. For LAH4-n, the free energy difference between the inserted state and the superficial orientation was (-40 ± 6) kJ mol^{-1}. By contrast, the two alignments were equally probable, within errors, for LAH4-c (-15 ± 20 kJ mol^{-1}). This result is in qualitative agreement with the minimum-bias findings: the standard free energy difference between inserted and superficial states estimated from the frequencies of these orientations in the SW simulations was (-2.5 ± 0.4) kJ mol^{-1} and (-0.3 ± 0.3) kJ mol^{-1} for LAH4-n and LAH4-c, respectively, with errors calculated according to a binomial statistics. Interestingly, also the peptide arrangements and conformations corresponding to the local minima of the free energy profile (Fig. 8) paralleled exactly those observed in the minimum bias simulations (Fig. 5).

4. Discussion

In agreement with the experimental data, all three computational approaches predicted a very different behavior for the two protonation states of LAH4. In the case of AA simulations, this accord between our simulations and experiments could be substantiated by several quantitative comparisons. The pH-dependent changes in alignment of the peptide with respect to the bilayer normal, which were monitored by solid-state NMR measurements in POPC membranes [37,39,41], also occurred in the MD simulation and good agreement, within experimental errors, was observed for the order parameters of backbone CO bonds and those determined in polarized ATR-FTIR measurements of the amide I vibrational transition [38] (Table 1). A significant lipid disordering effect was observed for LAH4-c only (Fig. 3) and this is in agreement with the results of solid-state NMR studies performed on several different systems [60–62]. Some degree of unfolding of the peptide helix was observed in the simulations of LAH4-c, either at the termini or in the middle of the sequence, with the formation of a hinge. These findings parallel nicely to what has been observed in the NMR structures of LAH4-c in micelles [40]. All these data support the validity of the observed structures.

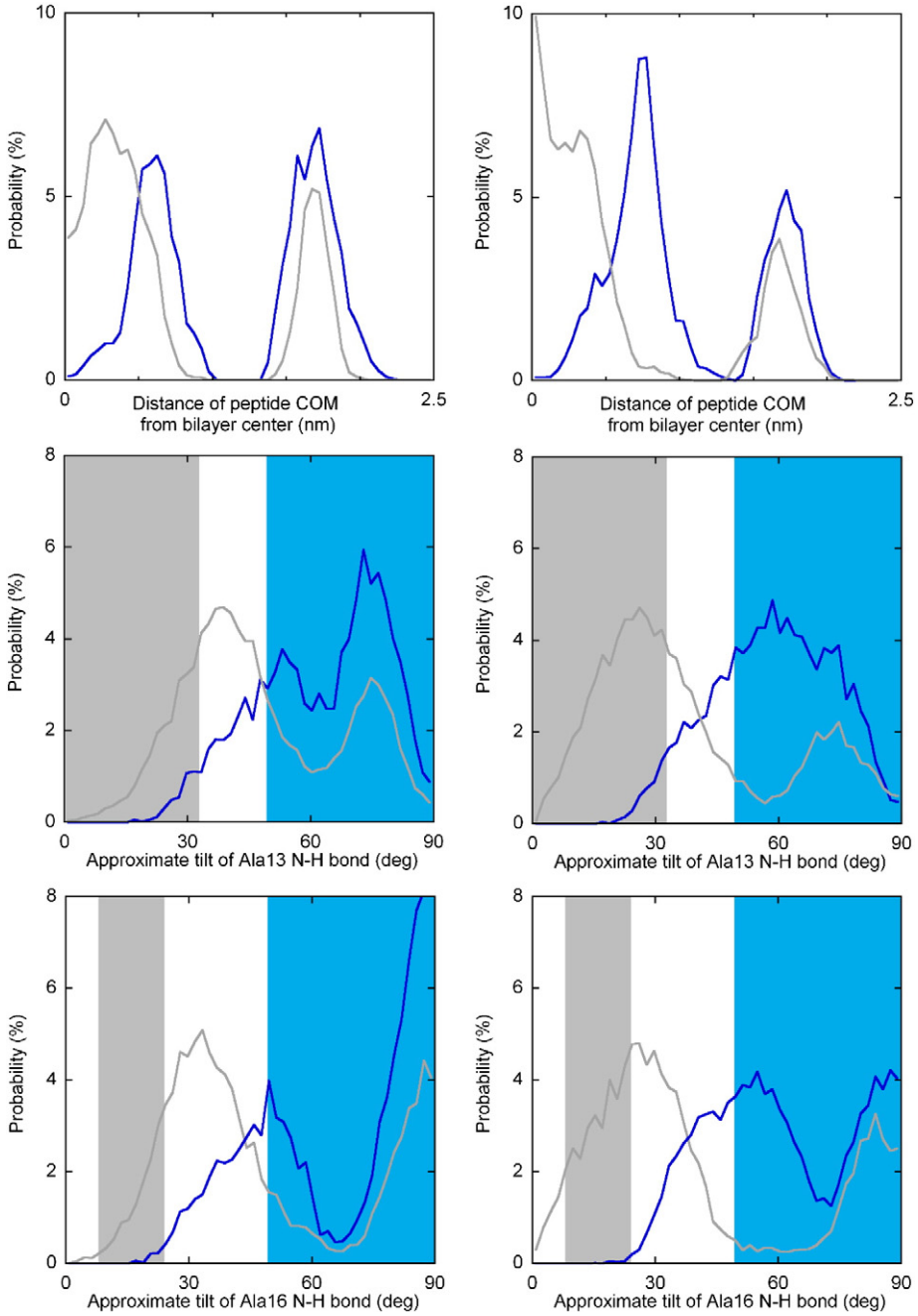

Fig. 6. Distributions of peptide position (top panels) and tilt (lower panels) in CG simulations performed with SW (left) and PW (right) model. Profiles were calculated in the last 20 ns of LAH4-n (gray) or LAH4-c (blue) simulations. Angle ranges, determined by NMR experiments on LAH4 at neutral and acidic pH values and by the restriction plot analysis reported in Fig. 3, are shown as gray and blue shaded areas, respectively.

The canonical TM orientation and conformation of LAH4-n predicted by our simulations are exactly what had been hypothesized based on the experimental data. However, most cationic amphipathic peptides similar to LAH4-c usually bind parallel to the membrane surface, just below the phospholipid headgroups. For instance, this was the position determined experimentally and observed in simulations similar to those reported here for PMAP-23 [22] and P5 [23]. By contrast, in our simulations LAH4-c stabilized membrane defects, by interacting through its charged residues with lipid headgroups of both leaflets (Fig. 2). This finding was rather surprising, since it was never observed in previous AA simulations of membrane self-assembly in the presence of a single membrane-active peptide molecule, performed by our group [2,22,23] and by others [24,26,28,64], with the single exception of protegrin-1 [65]. Usually, membrane defects can be easily healed and in the end the cationic peptide interacts with just one leaflet, binding close to the surface. Therefore, the ability to stabilize bilayer defects, by associating with both membrane surfaces, seems to be a peculiar property of some peptides, and might provide indications on their mode of membrane perturbation. The structures reported in Fig. 2 for membrane-bound LAH4-c are reminiscent of the interfacial activity model [66], where peptides with an imperfect amphiphilic arrangement of their side-chains cause membrane permeability by inserting some charged groups in the hydrophobic core of the membrane, thus drawing lipid polar headgroups and water molecules inside the bilayer. Indeed, LAH4-c is able to cause membrane leakage at the bound peptide to lipid ratio of 1/128 used in the simulations [39]. In addition, its helical structure is perfectly amphiphilic only in the central region, but not at the chain ends, and the terminal Lys residues appear to play a

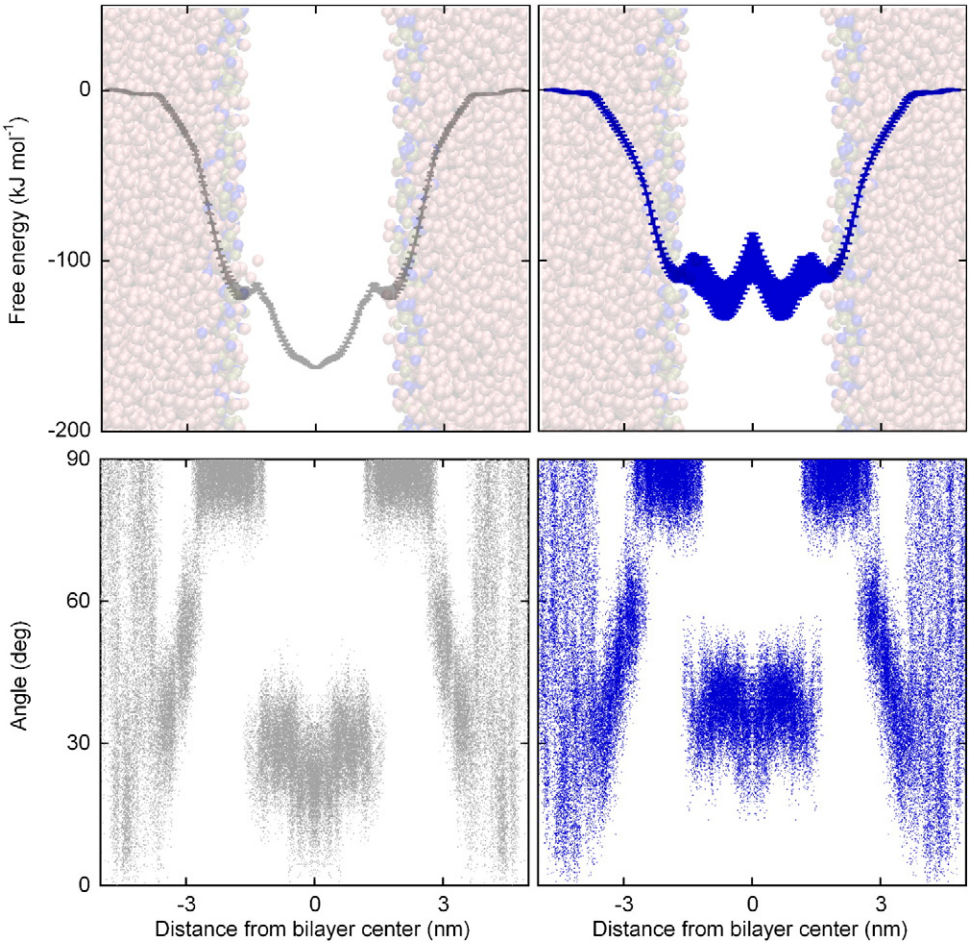

Fig. 7. PMF free-energy profiles (top) and tilt angle distributions (bottom) for the insertion of LAH4-n (left panels) and LAH4-c (right panels) in a POPC bilayer. The free energy profiles report averages and standard errors calculated from the three independent simulations of LAH4-n and LAH4-c. In the bottom plots, the tilt angles formed between the membrane normal and the helix axis (calculated by joining the center of mass of the three N-terminal and C-terminal backbone beads) are reported with a dot for each frame of the simulation, collected every 0.24 ns. All plots are symmetrized with respect to the membrane center.

fundamental role in stabilizing the membrane defects observed in the simulations. In principle, it might be argued that His residues, when inserted in the low dielectric medium of the membrane core, might become deprotonated even at low pH values. We cannot rule out the possibility that the fixed protonation state used in our simulations somehow biased the predicted structures. However, the apparent pK_a values of LAH4 His residues measured in a micellar environment are in the range 5.4 to 6, so that all side chains are protonated at pH around 4.5, where the orientational transition is complete. In addition, for Arg residues it has been convincingly demonstrated that membrane insertion of the protonated form is possible, thanks to the concomitant presence of phospholipid headgroups and water molecules [67], similar to what is happening in our simulations. The good agreement with the experimental results supports the conclusion that the observed structures are related to what is actually happening during membrane permeabilization by LAH4 in real membranes.

It is worth mentioning that the present findings are in striking contrast to those of a recent AA simulation study of LAH4, performed by starting with a preformed bilayer and the peptide in the water phase [44]. In that case, very superficial peptide positions were observed, irrespective of the His charge state, confirming that simulations of membrane-active peptides performed in the presence of preformed bilayers can suffer from significant sampling problems, related to the limited length of the simulated trajectories. The present investigation indicates that those limitations are strongly reduced in the case of the minimum-bias approach.

CG simulations of LAH4-n showed a strong prevalence for a transmembrane orientation, in agreement with both experimental data and AA simulations. We did observe also some in-plane alignments, but the occasional occurrence of less favorable peptide orientations is a common finding in CG self-assembly simulations [68,69]. Indeed, even for cationic peptides known to locate at the membrane surface, such as PMAP-23 and magainin, we observed a fraction of simulations resulting in inserted structures. These observations might be related to a potential effect of the minimum bias approach on the "roughness" of the free energy surface during the first stages of the simulation, enhanced by a similar influence of the CG approximation [20]. The effectiveness of this method in finding the peptide arrangements corresponding to free energy minima is due to the high mobility of the system in the first stages of the simulation, which precede the formation of a defect-free bilayer. This implies that the free energy differences and barriers between different peptide arrangements are likely smaller than in a fully formed membrane. Once the membrane defects are healed, the system might become "frozen" (on the MD time-scale) and the relative populations observed in minimum-bias simulations might somehow deviate from those determined in an equilibrated system. Even with these considerations, the behavior observed for LAH4-c was distinctive of this specific peptide, similarly to what was observed in the AA simulations. While other cationic AMPs attained a superficial arrangement in most of the CG simulations, for LAH4-c two different states (surface-bound and inserted) where equally populated. However, in this case the inserted arrangement was very different from the TM orientation

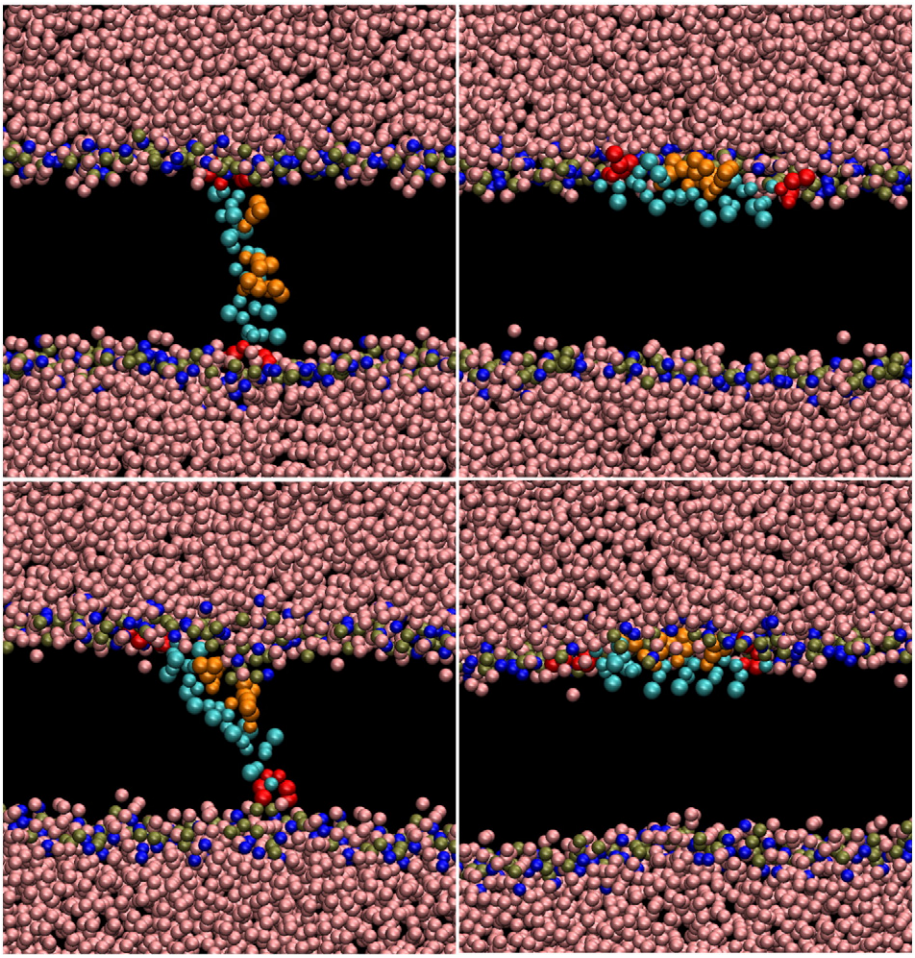

Fig. 8. Representative minimum free energy structures of LAH4-n (upper panels) and LAH4-c (lower panels). Left, structures corresponding to the inserted free energy minimum. The center of mass of the LAH4-n is located at the center of the bilayer, the helix axis forming an angle of 20° with the bilayer normal, while the center of mass of LAH4-c is 0.6 nm away from the bilayer center, with the helix axis tilted by 40° with respect to the bilayer normal. Right, structures corresponding to the superficial free energy minimum. The peptide is located at about 1.8 nm from bilayer center for both the His protonation states.

observed for LAH4-n, and resembled particularly one of the configurations observed in AA simulations of LAH4-c, with most charged residues interacting with one leaflet, and the two Lys at one of the termini reaching to the other layer of the membrane. The main difference between the AA and CG simulations of LAH4-c was that in the latter case membrane defects with lipid headgroups and water molecules inserted in the bilayer were not observed. This finding is very likely due to a well-known limitation of the CG MARTINI FF [20,70]. A detailed study [70] showed that the lack of defect formation is associated with the coarse graining of water (with one bead representing four water molecules) and more specifically with the parameters of the interaction potential between CG water and lipids. Unfortunately, until now it was not possible to find a set of parameters guaranteeing both a realistic formation of membrane pores, and the correct equilibrium proprieties of the membrane (*e.g.*, area per lipid) [70].

Solid-state NMR data exhibit a chemical shift for ^{15}N-lableled LAH4 of around 70–80 ppm under acidic conditions. The most straightforward interpretation of this finding is that LAH4-c attains a canonical surface bound arrangement only. However, restriction plot analysis showed that the two possible peptide orientations observed in the CG simulations of LAH4-c were in qualitative agreement with the published NMR data. Furthermore, recent experimental data indicated that subtle changes in the experimental conditions (buffer or lipid composition of the membrane) can significantly shift the orientational equilibrium of LAH4, with inserted states becoming favorable for LAH4 under acidic conditions in some cases, and superficial alignments prevailing for LAH4 in neutral environments in others [41]. Therefore, both in plane and inserted orientations correspond to local minima for LAH4 under both pH conditions. As a consequence, slight variations in the exact conditions, such as the relatively low water content of mechanically oriented samples in solid-state NMR experiments [71] or the presence of specific ions [41] might cause a significant variation in the relative populations of the two orientations. Overall, the minimum bias CG simulations were able to determine the structures corresponding to the free energy minima (see below), and indicated, consistently with AA results, that LAH4-c might be able to interact with headgroups of both lipid leaflets, thanks to its terminal Lys residues. This behavior might be an important aspect of the membrane-perturbing activity of LAH4 under acidic conditions.

Regarding the computational aspects, it is worth mentioning that the more sophisticated PW water model did not lead to any significant difference from the simpler SW approximation in the system under study. This finding is in agreement with a systematic comparison of the two water models showing that PW did not significantly improve the insertion of water in the membrane, while parameters for water-lipid interactions were critical [70]. These results suggest that the less computationally expensive SW is probably the most convenient choice for determining peptide location in membranes. Similarly, changing the specific starting peptide structure or the strength of the restraints on the backbone conformation did not modify the behavior of LAH4 in our simulations, confirming the robustness of our findings.

Having applied to LAH4 both the minimum bias self-assembly approach and PMF calculations with the CG FF, we can compare the two methods. The structures corresponding to the two free-energy local minima observed for each peptide state in the PMF profile were extremely similar to the structures and arrangements observed in the minimum bias simulations. Also the relative populations of the two states had the same trend in the two methods, with LAH4-c populating equally the two alignments, and LAH4-n preferring the TM orientation. However, in absolute terms, the free energy differences were significantly smaller in the minimum bias CG calculations. In the only other comparison of the two methods to have been published, to the best of our knowledge [69], a similar trend was observed. As discussed above, this might be a consequence of a smoother free energy surface in the first stages of minimum bias simulations, before a defect-free bilayer is formed. PMF profiles provide information also on the free energy of water-membrane partition, and on the free energy barriers for membrane translocation. For instance, in the present case PMF calculations predicted a free-energy difference between water and the membrane-bound minimum which was larger in the case of LAH4-n than for LAH4-c. This indicates a higher affinity for POPC membranes for the neutral-His peptide, in agreement with the difference observed experimentally in the apparent dissociation constants [39]. Therefore, hydrophobicity is important to provide membrane affinity, while charge facilitates bilayer perturbation.

The PMF approach is significantly more computationally demanding than minimum bias simulations: in the present instance, we simulated a total of 268 μs and 7 μs in the two cases, respectively. In addition, the computational cost of simulating each μs is greater in the case of the PMF systems, which comprised 5500 water beads, in comparison to the 1875 of the minimum bias simulations, needed in order to allow us to place the peptide entirely in the aqueous phase, with no interactions with the bilayer. Therefore, in all cases where water to membrane partition energies don't have to be estimated, and only the peptide position in the membrane must be determined, we suggest the minimum bias method as the most opportune choice, since both techniques lead to similar results. Even though AA PMF calculations were not performed in the present study, which was focused on relatively inexpensive computational methods available to most computational research groups, this conclusion is very likely valid also for AA force fields. In this case, PMF calculations become extremely demanding: in the present instance, AA simulations would have been more than 1800 times more expensive than CG, leading to a predicted requirement of about 1.2×10^6 CPU hours on an i7 2600 @3.4 GHz for a set of simulations analogous to the CG PMF study reported here. In addition, a recent study showed that simulations of several microseconds for each insertion depth are needed to achieve convergence in AA PMF calculations of peptide-membrane systems [32]. By contrast, in the case of our CG calculations convergence was essentially reached already in 100 ns. Similarly, in our minimum bias simulations, a defect-free bilayer was obtained after 200–300 ns and several annealing cycles for the AA simulations, while less than 100 ns at 300 K were sufficient with coarse graining. Also these observations are probably related to the well know property of CG force fields, which cause a smoothing of the free energy surface [20].

In conclusion, the different computational methods applied in the present study predicted peptide structures, positions and orientations in the membrane that were consistent with the extensive amount of experimental data collected on LAH4 over the years. Particularly, AA minimum bias simulations were in quantitative agreement with several measured parameters. When validated by comparison with experimental data, even relatively inexpensive computational approaches provide valuable atomic insight into the behavior and energetics of the system under study. In the present case, the simulations suggested a plausible mechanism of membrane destabilization by LAH4 with protonated His side-chains: thanks to its terminal lysines, which break the designed amphiphilicity of the central region of the helix carrying the charged histidines, the peptide could interact with the headgroups of both lipid leaflets, thus stabilizing membrane defects and causing leakage.

Acknowledgements

We are grateful to Christopher Aisenbrey for valuable discussions on the thermodynamics of LAH4 membrane interactions. This work was supported by the Italian Ministry of Education, University and Research (grant 2010NRREPL_008), the Italian Ministry of Foreign Affairs and International Cooperation and the Cineca Consortium (Italy). The financial contributions of the Agence Nationale de la Recherche (projects TRANSPEP 07-PCV-0018, ProLipIn 10-BLAN-731, membrane DNP 12-BSV5-0012 and the LabEx Chemistry of Complex Systems 10-LABX-0026_CSC), the Région Alsace (PhD grant to NV), and the RTRA International Center of Frontier Research in Chemistry are gratefully acknowledged.

Appendix A. Supplementary data

Supplementary data to this article can be found online at http://dx.doi.org/10.1016/j.bbamem.2014.11.002.

References

[1] B. Bechinger, K. Lohner, Detergent-like action of linear cationic membrane-active antibiotic peptides, Biochim. Biophys. Acta 1758 (2006) 1529–1539.
[2] G. Bocchinfuso, A. Palleschi, B. Orioni, G. Grande, F. Formaggio, C. Toniolo, Y. Park, K.-S. Hahm, L. Stella, Different mechanisms of action of antimicrobial peptides: insights from fluorescence spectroscopy experiments and molecular dynamics simulations, J. Pept. Sci. 15 (2009) 550–558.
[3] B. Bechinger, J.M. Resende, C. Aisenbrey, The structural and topological analysis of membrane-associated polypeptides by oriented solid-state NMR spectroscopy: established concepts and novel developments, Biophys. Chem. 153 (2011) 115–125.
[4] B. Bechinger, V. Vidovic, P. Bertani, A. Kichler, A new family of peptide-nucleic acid nanostructures with potent transfection activities, J. Pept. Sci. 17 (2011) 88–93.
[5] D.M. Copolovici, K. Langel, E. Eriste, U. Langel, Cell-penetrating peptides: design, synthesis, and applications, ACS Nano 8 (2014) 1972–1994.
[6] M. Bucciantini, S. Rigacci, M. Stefani, Amyloid aggregation: role of biological membranes and the aggregate–membrane system, J. Phys. Chem. Lett. 5 (2014) 517–527.
[7] R.M. Epand, Fusion peptides and the mechanism of viral fusion, Biochim. Biophys. Acta 1614 (2003) 116–121.
[8] G. Drin, B. Antonny, Amphipathic helices and membrane curvature, FEBS Lett. 584 (2010) 1840–1847.
[9] S. Bobone, A. Piazzon, B. Orioni, J.Z. Pedersen, Y.H. Nan, K.-S. Hahm, S.Y. Shin, L. Stella, The thin line between cell-penetrating and antimicrobial peptides: the case of Pep-1 and Pep-1-K, J. Pept. Sci. 17 (2011) 335–341.
[10] I. Moraes, G. Evans, J. Sanchez-Weatherby, S. Newstead, P.D. Stewart, Membrane protein structure determination — the next generation, Biochim. Biophys. Acta 1838 (2014) 78–87.
[11] U.H. Dürr, M. Gildenberg, A. Ramamoorthy, The magic of bicelles lights up membrane protein structure, Chem. Rev. 112 (2012) 6054–6074.
[12] G. Bocchinfuso, S. Bobone, C. Mazzuca, A. Palleschi, L. Stella, Fluorescence spectroscopy and molecular dynamics simulations in studies on the mechanism of membrane destabilization by antimicrobial peptides, Cell. Mol. Life Sci. 68 (2011) 2281–2301.
[13] S. Bobone, Y. Gerelli, M. De Zotti, G. Bocchinfuso, A. Farrotti, B. Orioni, F. Sebastiani, E. Latter, J. Penfold, R. Senesi, F. Formaggio, A. Palleschi, C. Toniolo, G. Fragneto, L. Stella, Membrane thickness and the mechanism of action of the short peptaibol trichogin GA IV, Biochim. Biophys. Acta 1828 (2013) 1013–1024.
[14] S. Ozdirekcan, C. Etchebest, J.A. Killian, P.F. Fuchs, On the orientation of a designed transmembrane peptide: toward the right tilt angle? J. Am. Chem. Soc. 129 (2007) 15174–15181.
[15] L. Monticelli, D.P. Tieleman, F.P. Fuchs, Interpretation of 2H-NMR experiments on the orientation of the transmembrane helix WALP23 by computer simulations, Biophys. J. 99 (2010) 1455–1464.
[16] Y. Wang, D.E. Schlamadinger, J.E. Kim, J.A. McCammon, Comparative molecular dynamics simulations of the antimicrobial peptide CM15 in model lipid bilayers, Biochim. Biophys. Acta 1818 (2012) 1402–1409.
[17] M. Pourmousa, J. Wong-Ekkabut, M. Patra, M. Karttunen, Molecular dynamic studies of transportan interacting with a DPPC lipid bilayer, J. Phys. Chem. B 117 (2013) 230–241.
[18] L. Monticelli, S.K. Kandasamy, X. Periole, R.G. Larson, D.P. Tieleman, S. Marrink, The MARTINI coarse-grained force field: extension to proteins, J. Chem. Theory Comput. 4 (2008) 819–834.
[19] S.J. Marrink, A.H. de Vries, A.E. Mark, Coarse grained model for semiquantitative lipid simulations, J. Phys. Chem. B 108 (2004) 750–760.
[20] S.J. Marrink, D.P. Tieleman, Perspective on the Martini model, Chem. Soc. Rev. 42 (2013) 6801–6822.

[21] P. Gkeka, L. Sarkisov, Interactions of phospholipid bilayers with several classes of amphiphilic alpha-helical peptides: insights from coarse-grained molecular dynamics simulations, J. Phys. Chem. B 114 (2010) 826–839.
[22] B. Orioni, G. Bocchinfuso, J.Y. Kim, A. Palleschi, G. Grande, S. Bobone, Y. Park, J.I. Kim, K.-S. Hahm, L. Stella, Membrane perturbation by the antimicrobial peptide PMAP-23: a fluorescence and molecular dynamics study, Biochim. Biophys. Acta 1788 (2009) 1523–1533.
[23] S. Bobone, G. Bocchinfuso, Y. Park, A. Palleschi, K.-S. Hahm, L. Stella, The importance of being kinked: role of pro residues in the selectivity of the helical antimicrobial peptide P5, J. Pept. Sci. 19 (2013) 758–769.
[24] S. Esteban-Martín, J. Salgado, Self-assembling of peptide/membrane complexes by atomistic molecular dynamics simulations, Biophys. J. 92 (2007) 903–912.
[25] P.J. Bond, D.L. Parton, J.F. Clark, M.S.P. Sansom, Coarse-grained simulations of the membrane-active antimicrobial peptide maculatin 1.1, Biophys. J. 95 (2008) 3802–3815.
[26] K. Wang, J. Yan, X. Liu, J. Zhang, R. Chen, B. Zhang, W. Dang, W. Zhang, M. Kai, J. Song, R. Wang, Novel cytotoxity exhibition mode of polybia-CP, a novel antimicrobial peptide from the venom of the social wasp *Polybia paulista*, Toxicology 288 (2011) 27–33.
[27] J.M. Crowet, D.L. Parton, B.A. Hall, S. Steinhauer, R. Brasseur, L. Lins, M.S.P. Sansom, Multi-scale simulation of the simian immunodeficiency virus fusion peptide, J. Phys. Chem. B 116 (2012) 13713–13721.
[28] K. Wang, J. Yan, W. Dang, X. Liu, R. Chen, J. Zhang, B. Zhang, W. Zhang, M. Kai, W. Yan, Z. Yang, J. Xie, R. Wang, Membrane active antimicrobial activity and molecular dynamics study of a novel cationic antimicrobial peptide *Polybia*-MPI, from the venom of *Polybia paulista*, Peptides 39 (2013) 80–88.
[29] C. Aisenbrey, P. Bertani, B. Bechinger, Solid-state NMR investigations of membrane-associated antimicrobial peptides, Antimicrobial Peptides Methods in Molecular Biology, 618, Humana Press, Springer, NY, 2010, pp. 209–233.
[30] A. Babakhani, A.A. Gorfe, J.E. Kim, J.A. McCammon, Thermodynamics of peptide insertion and aggregation in a lipid bilayer, J. Phys. Chem. B 112 (2008) 10528–10534.
[31] S. Yesylevskyy, S.J. Marrink, A.E. Mark, Alternative mechanisms for the interaction of the cell-penetrating peptides penetratin and the TAT peptide with lipid bilayers, Biophys. J. 97 (2009) 40–49.
[32] C. Neale, J.C. Hsu, C.M. Yip, R. Pomès, Indolicidin binding induces thinning of a lipid bilayer, Biophys. J. 106 (2014) L29–L31.
[33] P.J. Bond, C.L. Wee, M.S.P. Sansom, Coarse-grained molecular dynamics simulations of the energetics of helix insertion into a lipid bilayer, Biochemistry 47 (2008) 11321–11331.
[34] A. Chetwynd, C.L. Wee, B.A. Hall, M.S.P. Sansom, The energetics of transmembrane helix insertion into a lipid bilayer, Biophys. J. 99 (2010) 2534–2540.
[35] A. Kichler, C. Leborgne, J. März, O. Danos, B. Bechinger, Histidine-rich amphipathic peptide antibiotics promote efficient delivery of DNA into mammalian cells, Proc. Natl. Acad. Sci. U. S. A. 100 (2003) 1564–1568.
[36] A.J. Mason, C. Gasnier, A. Kichler, G. Prévost, D. Aunis, M.H. Metz-Boutigue, B. Bechinger, Enhanced membrane disruption and antibiotic action against pathogenic bacteria by designed histidine-rich peptides at acidic pH, Antimicrob. Agents Chemother. 50 (2006) 3305–3311.
[37] B. Bechinger, Towards membrane protein design: pH-sensitive topology of histidine-containing polypeptides, J. Mol. Biol. 263 (1996) 768–775.
[38] B. Bechinger, J.M. Ruysschaert, E. Goormaghtigh, Membrane helix orientation from linear dichroism of infrared attenuated total reflection spectra, Biophys. J. 76 (1999) 552–563.
[39] T.C. Vogt, B. Bechinger, The interactions of histidine-containing amphipathic helical peptide antibiotics with lipid bilayers. The effects of charges and pH, J. Mol. Biol. 274 (1999) 29115–29121.
[40] J. Georgescu, V.H. Munhoz, B. Bechinger, NMR structures of the histidine-rich peptide LAH4 in micellar environments: membrane insertion, pH-dependent mode of antimicrobial action, and DNA transfection, Biophys. J. 99 (2010) 2507–2515.
[41] B. Perrone, A.J. Miles, E.S. Salnikov, B.A. Wallace, B. Bechinger, Lipid interactions of LAH4, a peptide with antimicrobial and nucleic acid transfection activities, Eur. Biophys. J 43 (2014) 499–507.
[42] V.V. Vostrikov, B.A. Hall, M.S.P. Sansom, R.E. Koeppe II, Accommodation of a central arginine in a transmembrane peptide by changing the placement of anchor residues, J. Phys. Chem. B 116 (2012) 12980–12990.
[43] K. Witte, B.E.S. Olausson, A. Walrant, I.D. Alves, A. Vogel, Structure and dynamics of the two amphipathic arginine-rich peptides RW9 and RL9in a lipid environment investigated by solid-state NMR and MD simulations, Biochim. Biophys. Acta 1828 (2013) 824–833.
[44] M. Islami, F. Mehrnejad, F. Doustdar, M. Alimohammadi, M. Khadem-Maaref, M. Mir-Derikvand, M. Taghdir, Study of orientation and penetration of LAH4 into lipid bilayer membranes: pH and composition dependence, Chem. Biol. Drug Des. 84 (2014) 242–252.
[45] R. Macháň, P. Jurkiewicz, A. Olžyńska, M. Olšinová, M. Cebecauer, A. Marquette, B. Bechinger, M. Hof, Peripheral and integral membrane binding of peptides characterized by time-dependent fluorescence shifts: focus on antimicrobial peptide LAH4, Langmuir 30 (2014) 6171–6179.
[46] A. Kichler, J. Mason, B. Bechinger, Cationic amphipathic histidine-rich peptides for gene delivery, Biochim. Biophys. Acta 1758 (2006) 301–307.
[47] L. Prongidi-Fix, M. Sugawara, P. Bertani, J. Raya, C. Leborgne, A. Kichler, B. Bechinger, Self-promoted cellular uptake of peptide/DNA transfection complexes, Biochemistry 46 (2007) 11253–11262.
[48] B. Langlet-Bertin, C. Leborgne, D. Scherman, B. Bechinger, A.J. Mason, A. Kichler, Design and evaluation of histidine-rich amphipathic peptides for siRNA delivery, Pharm. Res. 27 (2010) 1426–1436.
[49] D. Fenard, S. Genries, D. Scherman, A. Galy, S. Martin, A. Kichler, Infectivity enhancement of different HIV-1-based lentiviral pseudotypes in presence of the cationic amphipathic peptide LAH4-L1, J. Virol. Methods 189 (2013) 375–378.
[50] S.J. Marrink, O. Berger, D.P. Tieleman, F. Jaehnig, Adhesion forces of lipids in a phospholipid membrane studied by molecular dynamics simulations, Biophys. J. 74 (1998) 931–943.
[51] S. Pronk, S. Páll, R. Schulz, P. Larsson, P. Bjelkmar, R. Apostolov, M.R. Shirts, J.C. Smith, P.M. Kasson, D. van der Spoel, B. Hess, E. Lindahl, GROMACS 4.5: a high-throughput and highly parallel open source molecular simulation toolkit, Bioinformatics 29 (2013) 845–854.
[52] D.H. de Jong, G. Singh, W.F.D. Bennett, C. Arnarez, T.A. Wassenaar, L.V. Schäfer, X. Periole, D.P. Tieleman, S.J. Marrink, Improved parameters for the martini coarse-grained protein force field, J. Chem. Theory Comput. 9 (2013) 687–692.
[53] S.J. Marrink, H.J. Risselada, S. Yefimov, D.P. Tieleman, A.H. de Vries, The MARTINI force field: coarse grained model for biomolecular simulations, J. Phys. Chem. B 111 (2007) 7812–7824.
[54] S.O. Yesylevskyy, L.V. Schäfer, D. Sengupta, S.J. Marrink, Polarizable water model for the coarse-grained MARTINI force field, PLoS Comput. Biol. 6 (2010) e1000810.
[55] G. Torrie, J. Valleau, Nonphysical sampling distributions in Monte Carlo free-energy estimation: umbrella sampling, J. Comput. Phys. 23 (1977) 187–199.
[56] S. Kumar, J.M. Rosenberg, D. Bouzida, R.H. Swendsen, P.A. Kollman, The weighted histogram analysis method for free-energy calculations on biomolecules. I. The method, J. Comput. Chem. 13 (1992) 1011–1021.
[57] M. Michalek, E.S. Salnikov, B. Bechinger, Structure and topology of the huntingtin 1–17 membrane anchor by a combined solution and solid-state NMR approach, Biophys. J. 105 (2013) 699–710.
[58] E. Salnikov, P. Bertani, J. Raap, B. Bechinger, Analysis of the amide (15)N chemical shift tensor of the C(alpha) tetrasubstituted constituent of membrane-active peptaibols, the alpha-aminoisobutyric acid residue, compared to those of di- and tri-substituted proteinogenic amino acid residues, J. Biomol. NMR 45 (2009) 373–387.
[59] P. Bertani, J. Raya, B. Bechinger, ^{15}N chemical shift referencing in solid state NMR, Solid State Nucl. Magn. Reson. 61–62 (2014) 15–18.
[60] N. Voievoda, Biophysical Investigations of the Membrane and Nucleic Acids Interactions of the Transfection Peptide LAH4–L1(PhD thesis) University of Strasbourg, 2014.
[61] A.J. Mason, A. Martinez, C. Glaubitz, O. Danos, A. Kichler, B. Bechinger, The antibiotic and DNA-transfecting peptide LAH4 selectively associates with, and disorders, anionic lipids in mixed membranes, FASEB J. 20 (2006) 320–322.
[62] A.J. Mason, C. Leborgne, G. Moulay, A. Martinez, O. Danos, B. Bechinger, A. Kichler, Optimising histidine rich peptides for efficient DNA delivery in the presence of serum, J. Control. Release 118 (2007) 95–104.
[63] B. Bechinger, M. Zasloff, S.J. Opella, Structure and orientation of the antibiotic peptide magainin in membranes by solid-state nuclear magnetic resonance spectroscopy, Protein Sci. 2 (1993) 2077–2084.
[64] H. Leontiadou, A.E. Mark, S.J. Marrink, Antimicrobial peptides in action, J. Am. Chem. Soc. 128 (2006) 12156–12161.
[65] S.K. Kandasamy, R.G. Larson, Binding modes of protegrin-1, a beta-strand antimicrobial peptide, in lipid bilayers, Mol. Simul. 37 (2007) 799–807.
[66] W.C. Wimley, Describing the mechanism of antimicrobial peptide action with the interfacial activity model, ACS Chem. Biol. 5 (2010) 905–917.
[67] K. Hristova, W.C. Wimley, A look at arginine in membranes, J. Membr. Biol. 239 (2011) 49–56.
[68] V.V. Vostrikov, B.A. Hall, D.V. Greathouse, R.E. Koeppe, M.S.P. Sansom, Changes in transmembrane helix alignment by arginine residues revealed by solid-state NMR experiments and coarse-grained MD simulations, J. Am. Chem. Soc. 132 (2010) 5803–5811.
[69] B.A. Hall, A.P. Chetwynd, M.S.P. Sansom, Exploring peptide-membrane interactions with coarse-grained MD simulations, Biophys. J. 100 (2011) 1940–1948.
[70] W.F.D. Bennett, D.P. Tieleman, Water defect and pore formation in atomistic and coarse-grained lipid membranes: pushing the limits of coarse graining, J. Chem. Theory Comput. 7 (2011) 2981–2988.
[71] C.M. Moraes, B. Bechinger, Peptide-related alterations of membrane-associated water: deuterium solid-state NMR investigations of phosphatidylcholine membranes at different hydration levels, Magn. Reson. Chem. 42 (2004) 155–161.

Molecular Dynamics Methods to Predict Peptide Locations in Membranes: LAH4 as a Stringent Test Case.

A. Farrotti,[1] G. Bocchinfuso,[1] A. Palleschi,[1] N. Rosato,[2,3] E. S. Salnikov,[4] N. Voievoda,[4] B. Bechinger,[4] L. Stella[1,*]

[1]Dipartimento di Scienze e Tecnologie Chimiche, [2]Dipartimento di Medicina Sperimentale e Chirurgia and [3]NAST center, Università di Roma "Tor Vergata", 00133, Rome, Italy.
[4]Université de Strasbourg / CNRS, Institut de Chimie UMR7177, F-67000 – Strasbourg, France.

* To whom correspondence should be addressed: stella@stc.uniroma2.it

SUPPLEMENTARY MATERIAL

Table S1. Parameters employed in CG simulations.[a]

Parameters		**Water model**	
		SW	*PW*
	dt (ps)	0.03	0.02
	rlist (nm)	1.2	1.2
Electrostatics	coulombtype	Shift	PME
	rcoulomb_switch (nm)	0	0
	rcoulomb (nm)	1.2	1.2
	epsilon_r	15	2.5
vdW	vdw_type	shift	shift
	rvdw_switch (nm)	0.9	0.9
	rvdw (nm)	1.2	1.2
T coupling	tcoupl	Berendsen	Berendsen
P coupling	pcoupl	Berendsen	Berendsen
	Pcoupltype	anisotropic	anisotropic

[a]The table reports the keywords used in the setting of the MD simulations in the GROMACS software package.

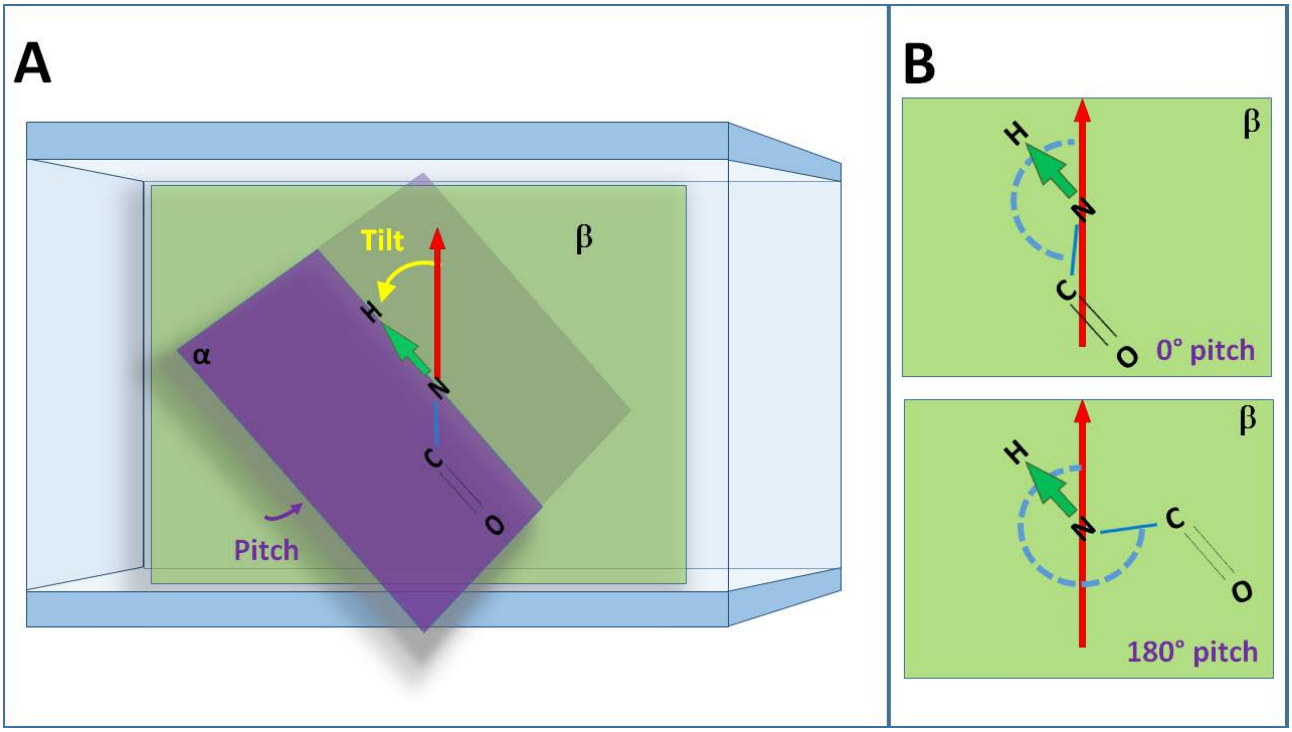

Figure S1. Definition of the tilt and pitch angles used in the analysis of peptide orientations inside lipid bilayers. A:Tilt is the angle formed by the N-H bond of the ^{15}N-labeled residue with the normal to the bilayer plane (coincident with the direction of the NMR magnetic field B_0), in the counterclockwise direction. It is measured in the plane individuated by these two vectors, and indicated as β in the figure. Pitch takes into account rotations of the labeled peptide bond plane around the N-H bond. Its value is defined as the angle formed by the plane of the peptide bond involving the labeled N atom (plane α) with the plane determined by the bilayer normal and the N-H bond (plane β), counted in a counterclockwise direction.

B: 0° pitch is defined as the orientation where the plane of the peptide bond (plane α) coincides with plane β. This still leaves an ambiguity, since 0° and 180° pitch fall on the same plane. To distinguish between these two possibilities, we define pitch=0° as the orientation where the N-C peptide bond forms the smaller angle (of the two possibilities) with the B_0 vector in the α≡β plane, counted in a counterclockwise direction. This angle is indicated by the light blue dashed lines in the figure.

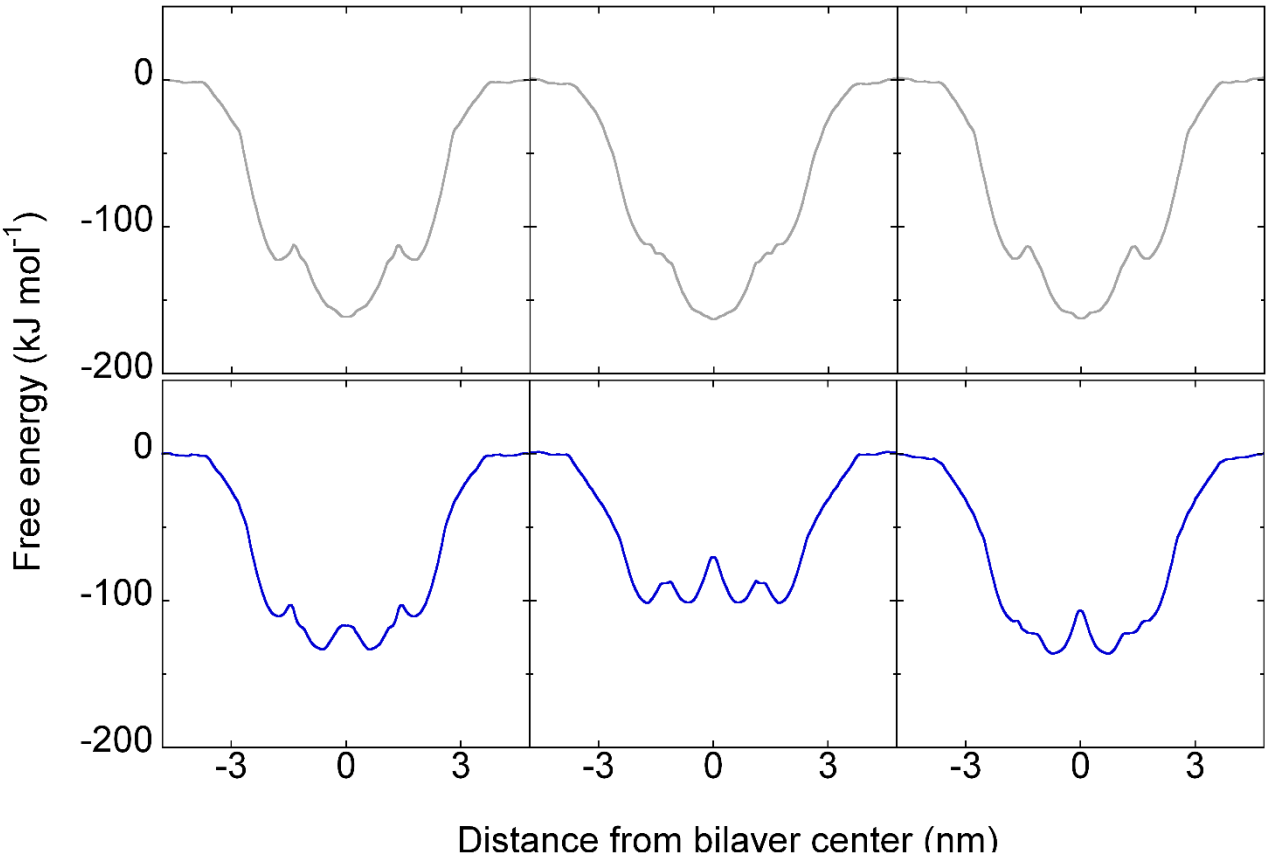

Figure S2. PMF free-energy profiles for the insertion of LAH4-n (upper panels) and LAH4-c (lower panels) in a POPC bilayer. Each panel reports a profile obtained from an independent simulation.

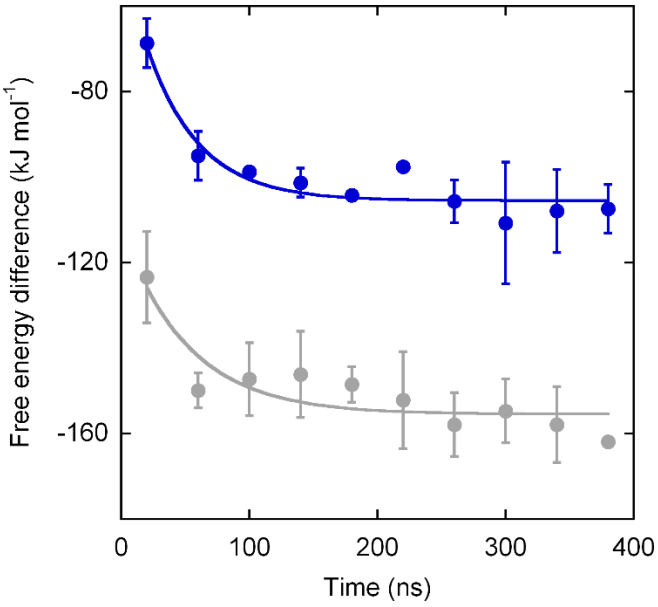

Figure S3. Convergence of PMF calculations. The free energy difference between the water phase and the absolute minimum in the PMF profile was calculated in different 40 ns time windows after the initial 60 ns equilibration. Gray: LAH4-n, blue: LAH4-c. Averages and standard deviations calculated on the three replicas are reported.